

RESEARCH

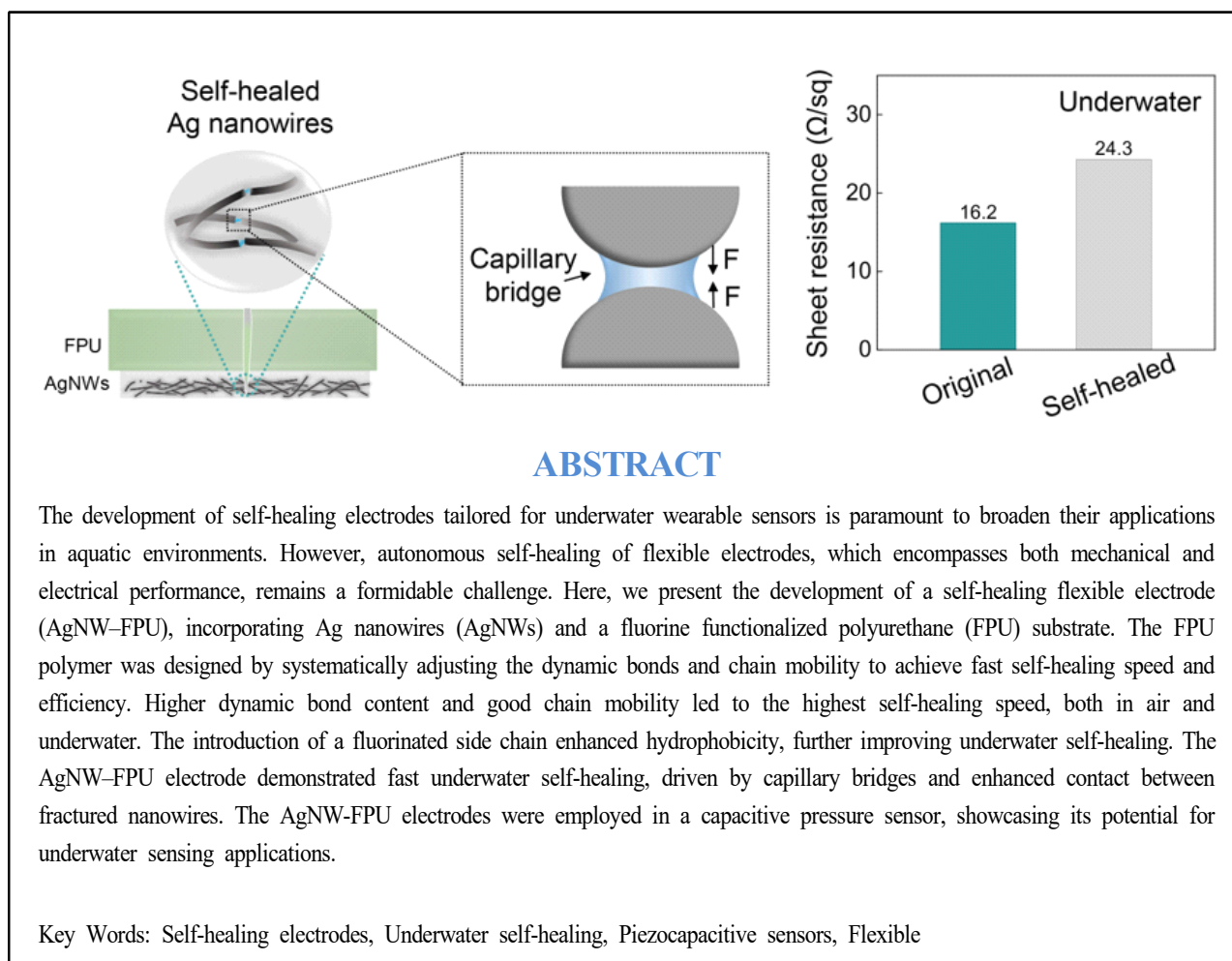
Autonomous Self-Healable, Ag Nanowire–Polymer Composite Flexible Electrode for Underwater Sensors

Zhengyang Kong^{1†}, Elvis K. Boahen^{1†}, Hayoung Lim¹, Do Hwan Kim^{1,2,3*}

¹Department of Chemical Engineering, Hanyang University, Seoul, Korea

²Institute of Nano Science and Technology, Hanyang University, Seoul, Korea

³Clean-Energy Research Institute, Hanyang University, Seoul, Korea



[†]These authors contributed equally to this work.

*Correspondence: dhkim76@hanyang.ac.kr



1. INTRODUCTION

The advancement of wearable sensor technology for flexible electronics has extended its reach to aquatic environments owing to the increasing demand for diverse applications in underwater robotics, underwater communication, and underwater animal tracking [1-3]. However, wearable sensors are susceptible to unpredictable mechanical damage owing to their soft nature, leading to a reduction in sensing capabilities or device failure. Notably, the integration of self-healing properties into wearable sensors, enabling structural or functional self-healing, is imperative to ensure the long-term stability and reliability of these devices [4]. Conventionally, water molecule absorption compromises the comprehensive underwater self-healing of polymer materials and electrodes owing to disruption of the dynamic bonds and conductive layers [5-7]. Several strategies have been taken to develop underwater self-healing polymer substrate and electrodes, however, restoring flexible electrodes, which encompasses both mechanical and electrical performance, remains a formidable challenge. Thus, the development of self-healing electrodes tailored for underwater wearable sensors is paramount to broaden their applications in aquatic environments.

Self-healing electrodes can be fabricated by incorporating conductive particles into a self-healing elastomer or by coating the elastomer surface with a conductive layer. For instance, the Bartlett group embedded a liquid metal network into a physically cross-linked styrene-isoprene-styrene block copolymer matrix, to create a self-healing metal composite material [8]. Our research group also leveraged a self-healing

polyurethane (PU) with dynamic disulfide bonds as the substrate and coated silver nanowires (AgNWs) on the substrate's surface to obtain a flexible electrode capable of fast self-healing at room temperature [9]. However, these approaches are restricted to self-healing exclusively in ambient air and are ineffective in aquatic environments due to the material's vulnerability to water molecule ingress, resulting in electrical interferences and short circuiting [10-11]. A few studies have also reported the development of water-insensitive flexible electrodes employing hydrophobic and self-healing elastomers as encapsulation layers. For instance, the Bao group engineered a flexible self-healing electrode comprising liquid metal EGaIn as the conductive layer and a hydrophobic self-healing PDMS-PU matrix as the encapsulation and support layer [12]. Similarly, the Haick group employed a hydrophobic and self-healing PU-based elastomer, embedding AgNWs or carbon nanotubes on its surface to fabricate a flexible self-healing electrode [13]. However, the limited self-healing driving force and suboptimal hydrophobic performance led to restricted self-healing efficiency and speed in aquatic environment, hindering the comprehensive restoration of the mechanical and electrical performance of the flexible electrodes. This limitation even resulted in a partial weakening of the sensor performance during prolonged recovery processes.

Herein, we present a self-healable electrode consisting of AgNW percolation network layer embedded in the surface of boronate ester-based self-healing PU matrix. The electrode composite possesses both structural and electrical self-healing in both ambient and aquatic environments without external stimuli. The PU



matrix features dynamic reversible boronate ester bonds for underwater self-healing by hydrolysis, and hydrophobic domains from high polar fluorocarbon groups (C-F), forming a barrier to repel the majority of interfacial water molecules [14]. A cut crack can quickly and efficiently self-heal in aqueous environment owing to the effective optimization of the hydrophobic domains allowing the ingress of small amount of water for effective hydrolysis by the boronate ester bonds. Concurrently, the AgNW percolation network on the PU's surface achieved self-healing, facilitated by the tractive self-healing force of the PU and capillary bridges formed by water droplets accumulation in the micro/nano gaps between AgNWs. Thus, the electrode exhibited sheet resistance as low as $27.2 \Omega/\text{sq}$ after self-healing, confirming effective restoration of electrical properties. Moreover, a mechanosensitive pressure sensor device was developed by sandwiching an iontronic sensor between two meticulously prepared electrodes to validate the electrode performance in wearable sensors. This composite electrode not only showcased remarkable underwater self-healing capabilities, but also demonstrated its substantial potential in the field of underwater sensors.

2. MATERIALS AND METHODS

2.1. Materials

Anhydrous tetrahydrofuran (THF, 99.5%), isophorone diisocyanate (IPDI, 99%), hydroxyl-terminated polybutadiene (HTPB, $M_n \approx 3,000 \text{ g mol}^{-1}$), and dibutyltin dilaurate (DBTDL, 98%) were purchased from Aladdin (China) and utilized without the need for further purification. Additionally, 1-butyl-3-methylim

idazolium bis(trifluoromethylsulfonyl)imide ([BMIM]⁺[TFSI]⁻, 98%), N,N-dimethylformamide (DMF, 99.8%), 1H,1H,2H,2H-perfluorodecylthiol (PFDT, 97%), and a 2,2'-azobis(2-methylpropionitrile) (AIBN) solution (0.2M in toluene) were purchased from TCI (Korea).

2.2. Design Principle of BPU

BPU were synthesized using a one-step polymerization method with GBDB, HTPB, and isophorone diisocyanate (IPDI), with dibutyltin dilaurate as a catalyst. To design different soft segment and hard segment ratios, five variants of GBDB weight were specified at 1 g, 1.5 g, 2 g, 2.5 g, and 3 g, respectively, based on a 10g HTPB reference (Supplementary Table S1). Consequently, this process yielded five distinct BPUs denoted as BPU-1, BPU-2, BPU-3, BPU-4, BPU-5.

2.3. Design Principle of BPU

In a glovebox saturated with 99.999% Ar, the reactants HTPB, chain extender GBDB, catalyst DBTDL, and anhydrous THF solvent were introduced into a three-necked reactor equipped with a mechanical stirrer. Following the complete dissolution of the reactants in the solvent, IPDI was introduced using a vacuum syringe. The reaction proceeded under heating at 65°C for 6 hours. All reactants maintained a weight concentration of 45 wt%, with DBTDL at a weight concentration of 1 wt%. The desired product underwent several washes with methanol, precipitation, and subsequent drying in a vacuum oven at 60°C for 24 hours, resulting in the formation of BPU (Supplementary Fig. S1). Similarly, FPU (Supplementary Fig. S2(b)) was synthesized under identical conditions as



described above except that HTPB was substituted with a synthesized mHTPB (comprising C-F group functionalization).

2.4. Fabrication of Self-Healing Electrodes

Various concentrations of the AgNW solutions were spray-coated (SRC-200 VT, E-FLEX, Korea; nozzle: 0.05 mm, pressure: 200 mbar) onto a polytetrafluoroethylene (PTFE, Teflon) mold and subjected to a 30 min heat treatment at 90°C to ensure the evaporation of excess IPA solution, thereby diminishing the resistance between nanowires. Subsequently, self-healable PU solution was drop-cast onto the PTFE mold coated with AgNW, followed by annealing at 65°C to transfer the AgNW percolation network. The film was then peeled off from the PTFE mold to obtain the AgNW-FPU composite electrode. The sheet resistance was measured using a four-point probe (AiT, CMT-100MP).

2.5. Characterization

The mechanical properties of BPU at room temperature were investigated using a universal testing machine (UTM, Instron 5567). Strain rates were controlled at 50 mm min⁻¹ with a dumbbell-shaped specimen measuring 35 mm (length), 2 mm (width), and approximately 0.5 mm (thickness). Young's modulus was determined based on the slope of the stress-strain curve (0-5% strain). Water contact angle (WCA) analysis was performed using a contact angle goniometer (OCA25, DataPhysics, Germany). The self-healing experiments were executed under both ambient conditions (20-40% relative humidity) and underwater conditions (deionized water) using an optical micro-

scope (Olympus/BX 51TF Instec H601, Japan) and Scanning Electron Microscopy (SEM; Apreo S Hivac). Thin film samples, with a thickness of 0.2 millimeters, were cut into two pieces and reconnected to assess self-healing capabilities. To investigate the response of the AgNW-FPU electrode-based piezocapacitive sensor, the device was connected to a precision LCR meter (Agilent Keysight Technologies, E4980A) to record capacitance changes.

3. RESULTS AND DISCUSSION

3.1. The Design Concept and Fabrication of Self-Healing Flexible Electrode for Underwater Sensors

To ensure the stable and secure deployment of wearable sensors in aquatic environments, adhesive-bonded encapsulation layers are commonly utilized to prevent the electrode's interference from water molecules [15-16]. Notably, self-healing PU elastomers can serve as an encapsulation layer without the need for adhesives, thereby facilitating high device integration. Thus, we developed a self-healing fluorine functionalized PU (FPU) elastomer, which not only shielded the electrodes and the iontronic sensor from excessive water ingress, but also facilitated rapid underwater self-healing capabilities (see section 3.2 for details). Specifically, we introduced reversible dynamic boronic ester bonds and highly polar C-F groups into the PU matrix (Fig. 1(a), left side) to achieve a flexible substrate with high self-healing speed by regulating water ingress. Upon accidental damage, the crack in the PU elastomer undergoes reconnection and self-healing facilitated by the reversible dynamic bonds and enhanced chain mobility. Simultaneously, the conductive

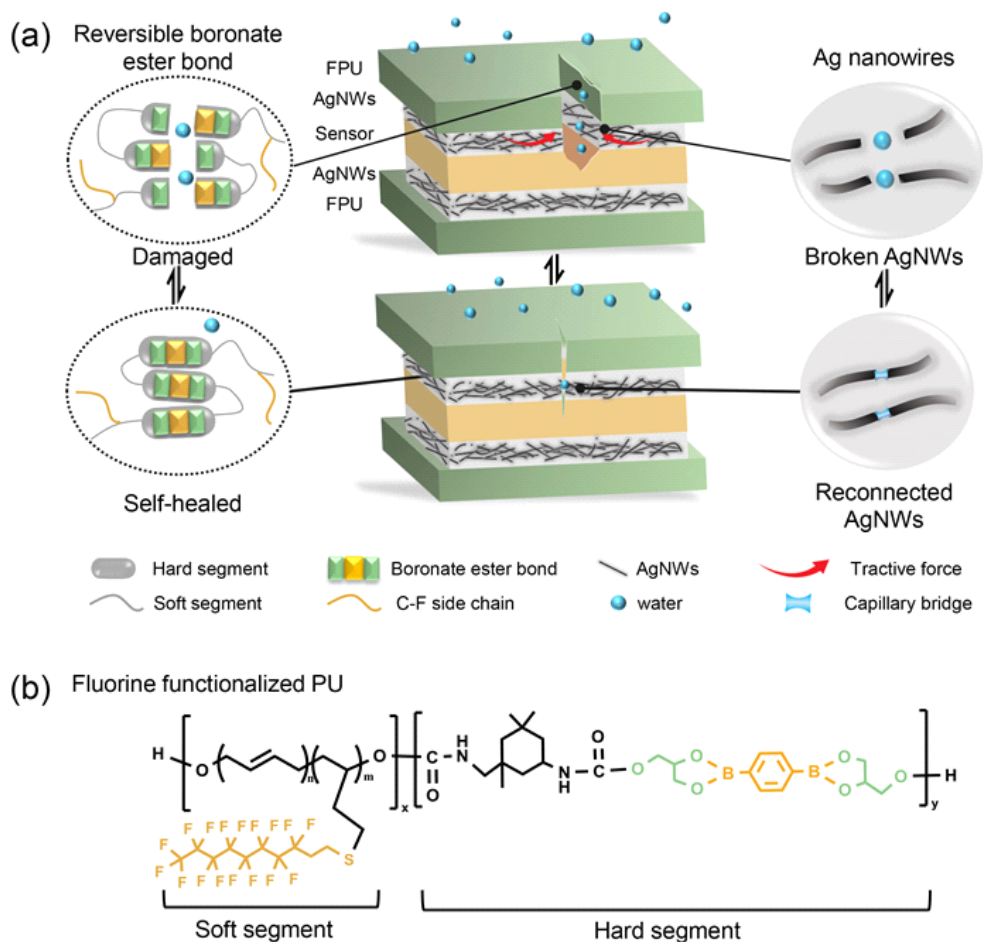


Fig. 1. (a) Conceptual design principle of underwater self-healing AgNW-FEPU composite flexible electrode. (b) Representation of the design chemistry of FEPU.

AgNW percolation network on the PU elastomer's surface achieved self-healing owing to the tractive force propagated by the self-healing driving force of FPU matrix connecting the cracked area [17]. Additionally, the regulated water molecules' entry generated capillary bridges in narrow gaps between neighboring AgNW network (Fig. 1(a), right side), which elevated the level of aggregation, ensuring effective reconstruction of the conductive network [18]. Fig. 1c shows the chemical structure of FPU consisting of side chain functionalized C-F groups and boronate ester

bonds.

3.2. Synthesis and Characterization of Various PUs

The self-healing capability of a flexible substrate represents a pivotal performance factor for self-healing flexible electrodes. Typically, elastomers comprise high chain rigidity and intermolecular interactions to achieve excellent mechanical properties [19-20]. However, these characteristics are contradictory to the high chain mobility required for efficient self-healing. Therefore, for applications in wearable sensors, the de-



elongation at break with an increasing content of hard segments, emphasizing the contribution of the hard segment region as a physical cross-linking point for achieving high mechanical properties. Therefore, in this system, the reduction in chain mobility of BPUs implies an increase in the content of dynamic bonds. The calculated self-healing speeds for BPU-1 to BPU-5 in air and underwater are depicted in Fig 2b. In air, the self-healing speed of various PUs increases with the content of dynamic bonds, except for a drastic decrease in BPU-5, with the highest dynamic bond content, owing to its relatively low chain mobility. Therefore, based on a higher dynamic bond content and relatively good chain mobility, BPU-4 achieves the highest self-healing speed. It is noteworthy that the self-healing speed of all BPUs in water is significantly higher than in air (Fig 2(b)). This can be attributed to the reversible boronate ester hydrolysis under the influence of small quantity of water molecules, as facilitated by the hydrophobicities of the various PUs (Fig. 2(c)). Nonetheless, in the event of excessive water entering the system, the boronate ester groups experience complete hydrolysis or dissociation, resulting in the formation of irreversible boronic acids and diols [21]. This situation impedes the possibility of re-esterification during the self-healing process. Therefore, it is essential to achieve a combined effect of relative hydrophobicity in order to control water ingress, which is necessary to enable the formation of reversible boronate ester bonds/re-esterification (Fig. 2(d)) and achieve exceptional self-healing properties in underwater conditions. However, increasing the content of HTPB, which comprises the hydrophobic component necessary to prevent complete hydrolysis or dissociation of

boronate esters, results in lower self-healing speed owing to limited dynamic bonds (Fig. 2(b)).

Therefore, FPU was fabricated by employing a C-F side chain engineering approach to enhance hydrophobicity while maintaining high dynamic bonds (Fig. 1(b) and Supplementary Fig. S2). FPU exhibits high hydrophobicity due to the high polarity of fluorinated groups and their weak interaction with water molecules (Fig. 2(e)). Moreover, as shown in Fig. 2(e), compared to BPU-4, FPU exhibits faster self-healing speed (5.8 $\mu\text{m}/\text{min}$) in air owing to dipole-dipole interaction between fluorinated groups [22]. Additionally, FPU demonstrates significantly superior underwater self-healing speed (16.2 $\mu\text{m}/\text{min}$) owing to effective hydrolysis/re-esterification reaction of boronate ester bonds, making it more suitable for the development of underwater self-healing flexible electrodes. To evaluate the self-healing performance of FPU, the macroscopic self-healing process was studied under an optical microscope in both ambient and aqueous environment. As depicted in Fig. 2(f), cut tests were conducted to evaluate the autonomous self-healing capabilities. The scars disappeared completely within 32 min in air (RH 20-40%), and within 12 min underwater at room temperature. The self-healing speed can be calculated using Equation (1):

$$\text{Self-healing speed} = \frac{\text{Notch size } (\mu\text{m})}{\text{Self-healing time (min)}} \times 100 \quad (1)$$

3.3. Exploration of the Reconnection Mechanism and Factors Influencing the Self-Healing of AgNWs Conductive Network

AgNWs, characterized by their remarkable flexi-



bility, high conductivity, and excellent solution processability, have emerged as highly promising candidates for flexible conductive materials [23]. The self-healable AgNW-FPU electrodes were fabricated through a process involving the spray coating of a AgNWs dispersed in acetone, onto a Teflon mold, followed by the drop-casting of FPU solution and annealing under optimized conditions, as depicted in Fig. 3(a). This process resulted in the transfer of the AgNW network onto the FPU substrate, which was subsequently peeled off from the Teflon mold to form the AgNW-FPU composite electrode. The electrical properties of the AgNW network are influenced by factors such as

the interconnection between individual nanowires and their concentration on the substrate [24]. The electrical self-healing of damaged electrodes in air is attributed to the reconnection of the conductive network as the FPU substrate undergoes self-healing, as illustrated in Fig. 3(b). During the healing process, the damaged AgNW percolation network achieves reconnection owing to the tractive force propagated by the self-healing driving force of FPU matrix connecting the cracked area. The reconnection process of the damaged AgNWs network was observed using Scanning Electron Microscopy (SEM). Fig. 3(c) displays cut and healed images of the electrode where the clearly bifurcated stacked

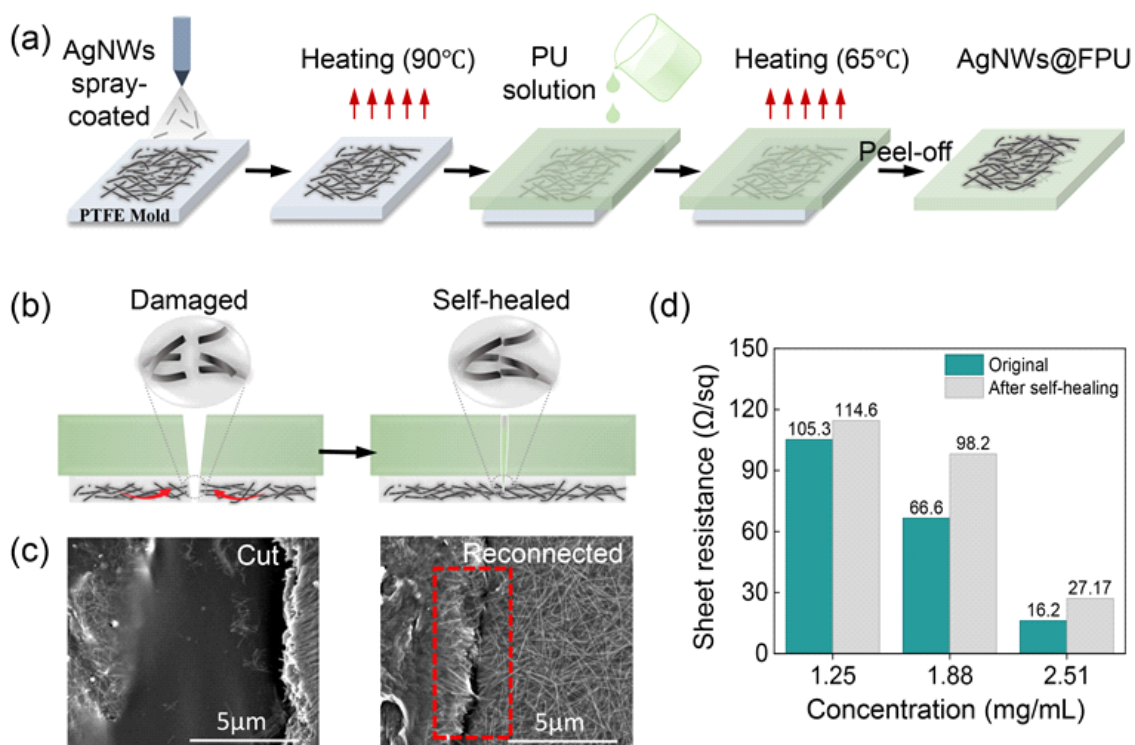


Fig. 3. (a) The fabrication method of self-healable AgNW-FPU electrodes. (b) The mechanism scheme of self-healable AgNW-FPU electrodes in air. (c) SEM images of AgNW-FPU electrodes before and after self-healing in air. (d) Sheet resistance of AgNW-FPU electrodes with different concentrations of AgNW before and after self-healing in air.



layers of AgNW network achieved reconnection after self-healing.

Additionally, the conductivity of the AgNW network is contingent on its concentration; higher concentrations lead to an increased number of AgNWs, resulting in a high-density nanowire network that facilitates low sheet resistance. Therefore, various concentrations of AgNWs solutions (1.25 mg/mL, 1.875 mg/mL, 2.5 mg/mL) were prepared to determine the lowest sheet resistance of the AgNW network for optimum electrical performance. The electrode with the highest concentration of AgNWs exhibited the lowest

sheet resistance of 16.2 Ω/sq (Fig. 3(d)). Furthermore, a self-healed network exhibited sheet resistance of 27.2 Ω/sq , depicting a minimal change after healing, which confirms the successful reconnection of the damaged network.

Moreover, the underwater self-healing mechanism of the AgNW percolation network was also explored. As depicted in Fig. 4(a), following damage to the percolation network, minute water droplets ingress through the FPU incision. As the incision gradually disappears with the self-healing of the FPU matrix, the disconnected conductive network re-establishes contact.

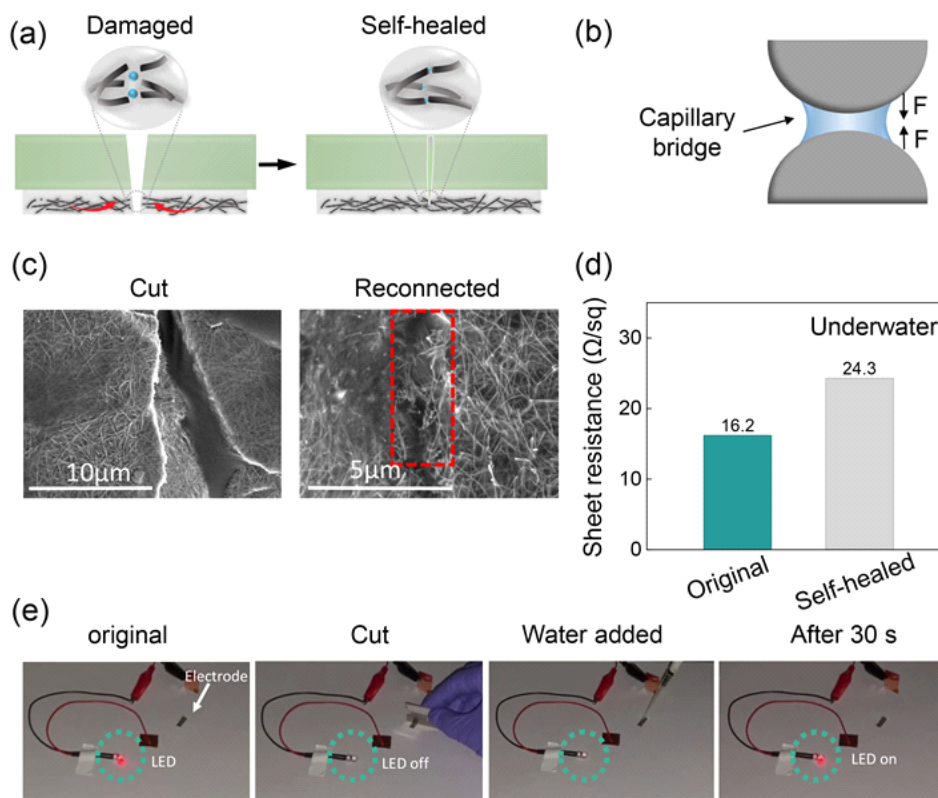


Fig. 4. (a) The mechanism scheme of self-healable AgNW-FPU electrodes in water. (b) Schematic diagram of capillary bridge. (c) SEM images of AgNW-FPU electrodes before and after self-healing in water. (d) Sheet resistance of AgNW-FPU electrodes with 2.51 mg/mL of AgNW before and after self-healing in water. (e) Demonstration of the electrical self-healing of electrodes in water using an LED.



Importantly, the minute water droplets accumulated in the micro/nano gaps between AgNWs, form capillary bridges in the narrow gaps, as illustrated in Fig. 4(b) [25]. Capillary forces, driven by Laplace pressure at the nanoscale, lead to the aggregation of AgNWs [18]. Additionally, droplets reestablish some fractured and loose AgNWs, facilitating their reconnection. Therefore, compared to self-healing in air, the AgNWs network exposed to a small amount of water exhibits stronger aggregation and more effective contacts, enabling the efficient reconstruction of the conductive network. SEM images demonstrate that the originally damaged AgNW network exhibits shallower and narrower scars after underwater self-healing compared to healing in air, confirming the activities of capillary forces in creating a dense AgNWs network, as shown in Fig. 4(c). The minimal difference in sheet resistance before ($16.2 \Omega/\text{sq}$) and after ($24.3 \Omega/\text{sq}$) underwater self-healing further supports the efficiency of healing of the AgNWs network in an aqueous environment (Fig. 4(d)). Additionally, the electrode was connected to a light-emitting diode (LED) to visualize the electrical self-healing process. After being cut across the width with a sharp blade, the LED intensity dimmed completely owing to damage to the AgNW percolation network. Within 30 s, the LED intensity was restored, confirming the self-healing capabilities of the electrodes (Fig. 4(e)).

3.4. Underwater Application Demonstration of a Flexible Electrode

To demonstrate the potential underwater applications of the AgNW-FPU electrode, we integrated it with an iontronic sensor to fabricate a piezocapacitive pressure

sensitive device. The piezocapacitive device was fabricated by sandwiching the iontronic sensor between two deformable self-healing AgNW-FPU electrodes (Fig. 5(a)). The iontronic sensor was developed using FPU and 30 wt% [BMIM][TFSI] ionic liquid. This sensor material exhibits dynamic ion-dipole interactions, stemming from the interaction between high polar C-F groups and [BMIM] cation, resulting in a dynamic ion trap and release phenomenon, as illustrated in Fig. 5(b) [9, 26]. Iontronic sensor materials that exhibit trap and release behavior often demonstrate exceptional sensitivity and high noise immunity, enabling a broad pressure sensing range [27]. At pre-stimulus, the majority of $[\text{BMIM}]^+[\text{TFSI}]^-$ ion pairs are trapped to the C-F groups with restricted mobility. However, under stimulus such as pressure, the device gradually undergoes deformation, reducing the distance between the top and bottom electrodes, generating a strong electric field as depicted in Fig. 5(b). This deformation, along with the pressure-induced breaking of ion-dipole interactions, leads to the dissociation of ion pairs from the C-F groups, facilitating the formation of Electric Double Layer (EDL) at the interface between the electrode and electrolyte. The mechanosensitive tactile sensor device was connected to an LCR meter to assess its underwater sensing capability, as depicted in Fig. 5(c). Applying light, medium, and strong touch forces generated corresponding weak, medium, and strong signals, as demonstrated in Fig. 5(d). Even after cutting the sensor with a single-edged blade and allowing it to undergo self-healing, the sensor continued to produce distinct signals for the three touch intensities, as shown in Fig. 5(e). This underscores the remarkable underwater sensing

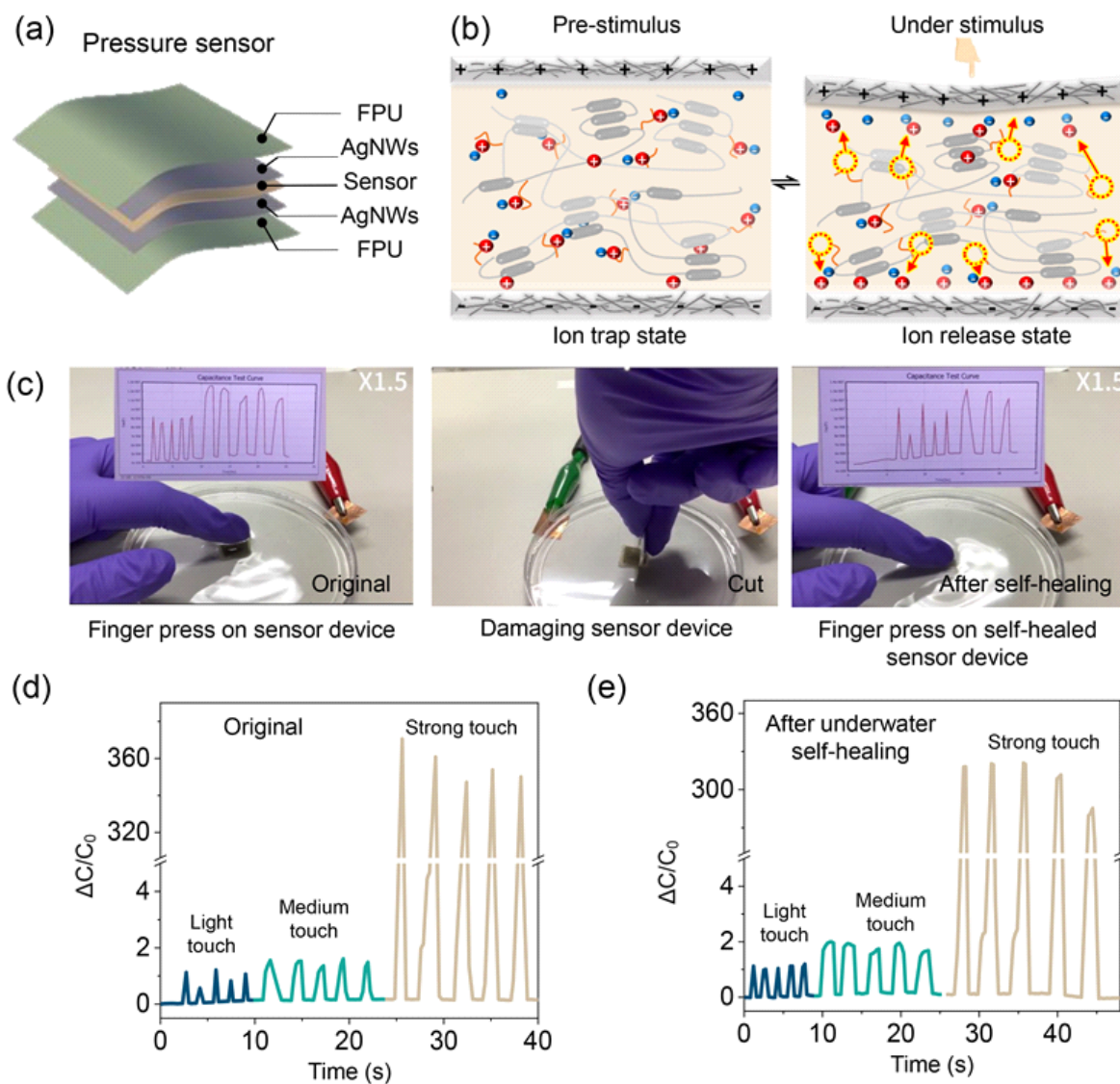


Fig. 5. (a) Illustration of AgNW-FPU electrodes-based pressure sensor device architecture comprising of iontronic sensor sandwiched between two deformable AgNW-FPU electrodes. (b) At a pre-stimulus condition, ions are trapped to C-F groups (trapped state). Under stimulus, iontronic sensor exhibits ion pumping phenomenon owing to pressure induced breaking of ion-dipole interactions. (c) Photographs showing the responses upon pressing with finger before and after self-healing in water. Sensing responses upon pressing with finger (d) before and (e) after self-healing in water.

and self-healing capabilities of the flexible electrode and iontronic sensor. These demonstrations highlight the significant potential of AgNW-FPU flexible electrodes for underwater wearable sensors.

4. CONCLUSION

In conclusion, we have successfully developed self-healing flexible electrode by integrating AgNWs



with FPU, demonstrating fast self-healing capabilities in both air and underwater environments. By adjusting the dynamic bond content and enhancing hydrophobicity, FPU achieved remarkable self-healing efficiency. The AgNW network exhibited rapid underwater self-healing, enabled by capillary bridges, and improved contact between fractured nanowires, ensuring minimal changes in electrical performance. Furthermore, two AgNW-FPU electrodes were successfully integrated into a capacitive pressure sensor, highlighting its potential for underwater touch response and sensing applications. This research contributes to the development of robust and versatile electrodes for the next generation of flexible electronics in aquatic environments.

ABBREVIATIONS

AgNW: Silver nanowire
PU: Polyurethane
FPU: Fluorine functionalized polyurethane
BPU: Boronate-based polyurethane
C-F: Fluorocarbon groups
GBDB: Glyceryl benzenediborate
HTPB: Hydroxyl-terminated polybutadiene
SEM: Scanning Electron Microscopy

SUPPLEMENTARY INFORMATION

The online version contains supplementary material available at <https://doi.org/10.56767/jfpe.2023.2.2.6>

ACKNOWLEDGEMENTS

Author Contributions

D.H.K. supervised the project. Z.K. prepared and

synthesize the materials. E.K.B. and Z.K. were involved in experiments, analysis, and discussion. H.L. assisted with the schematics and figure-sets. E.K.B. and Z.K. wrote the manuscript and D.H.K. revised the manuscript. All authors discussed the results and approved the manuscript.

Funding

This work was supported by the National R&D Program through the National Research Foundation of Korea (NRF) funded by the Ministry of Science and ICT (2021M3H4A1A03049075, 2022M3C1A3081211, and 2022M3H4A1A02076825). This work was also supported by the Basic Science Research Program of the National Research Foundation of Korea (NRF) funded by the Ministry of Science and ICT (2020R1A2C3014237), and the framework of international cooperation program managed by the National Research Foundation of Korea (2022K2A9A2A06046004)

Declarations of Competing Interests

The authors declare that they have no competing interests.

REFERENCES

- [1] Wei, J.; Zheng, Y.; Chen, T. A Fully Hydrophobic Ionogel Enables Highly Efficient Wearable Underwater Sensors and Communicators. *Mater. Horizons*. 2021, 8 (10), 2761-2770.
- [2] Wang, S.; Li, S.; Wang, H.; Lu, H.; Zhu, M.; Wu, X. E. et al. Highly Adhesive Epidermal Sensors with Superior Water-Interference-Resistance for Aquatic Applications. *Adv. Funct. Mater.* 2023,



- 2302687.
- [3] Yu, Z.; Wu, P. Underwater Communication and Optical Camouflage Ionogels. *Adv. Mater.* 2021, 33 (24), 2008479.
- [4] Chen, C.; Ying, W. B.; Li, J.; Kong, Z.; Li, F.; Hu, H. et al. A Self-Healing and Ionic Liquid Affiliative Polyurethane toward a Piezo 2 Protein Inspired Ionic Skin. *Adv. Funct. Mater.* 2022, 32 (4), 2106341.
- [5] Yu, Z.; Wu, P. Water-Resistant Ionogel Electrode with Tailorable Mechanical Properties for Aquatic Ambulatory Physiological Signal Monitoring. *Adv. Funct. Mater.* 2021, 31 (51), 2107226.
- [6] Sun, G.; Jiang, Y.; Sun, H.; Wang, P.; Meng, C.; Guo, S. Flexible, Breathable, and Hydrophobic Iontronic Tactile Sensors Based on a Nonwoven Fabric Platform for Permeable and Waterproof Wearable Sensing Applications. *ACS Appl. Electron. Mater.* 2023.
- [7] Huynh, T. P.; Khatib, M.; Haick, H. Self-Healable Materials for Underwater Applications. *Adv. Mater. Technol.* 2019, 4 (9), 1900081.
- [8] Tutika, R.; Haque, A. T.; Bartlett, M. D. Self-Healing Liquid Metal Composite for Reconfigurable and Recyclable Soft Electronics. *Commun. Mater.* 2021, 2 (1), 64.
- [9] Boahen, E. K.; Pan, B.; Kweon, H.; Kim, J. S.; Choi, H.; Kong, Z. et al. Ultrafast, Autonomous Self-Healable Iontronic Skin Exhibiting Piezo-Ionic Dynamics. *Nature Commun.* 2022, 13 (1), 7699.
- [10] Cao, Y.; Wu, H.; Allec, S. I.; Wong, B. M.; Nguyen, D. S.; Wang, C. A Highly Stretchy, Transparent Elastomer with the Capability to Automatically Self-Heal Underwater. *Adv. Mater.* 2018, 30 (49), 1804602.
- [11] Li, M.; Liu, Z.; Hu, Y.; Cao, Y. A Hydrophobic Eutectogel with Excellent Underwater Self-Adhesion, Self-Healing, Transparency, Stretchability, Ionic Conductivity, and Fully Recyclability. *Chem. Eng. J.* 2023, 472, 145177.
- [12] Kang, J.; Son, D.; Wang, G. J. N.; Liu, Y.; Lopez, J.; Kim, Y.; Oh, J. Y. et al. Tough and Water-Insensitive Self-healing Elastomer for Robust Electronic Skin. *Adv. Mater.* 2018, 30 (13), 1706846.
- [13] Khatib, M.; Zohar, O.; Saliba, W.; Srebnik, S.; Haick, H. Highly Efficient and Water-Insensitive Self-Healing Elastomer for Wet and Underwater Electronics. *Adv. Funct. Mater.* 2020, 30 (22), 1910196.
- [14] Cao, Y.; Tan, Y. J.; Li, S.; Lee, W. W.; Guo, H. C.; Cai, Y. Q. et al. Self-healing Electronic Skins for Aquatic Environments. *Nat. Electron.* 2019, 2 (2), 75-82.
- [15] Lin, H.; Zhang, C.; Liao, N.; Zhang, M., Micro-cracked Strain Sensor Based on Carbon Nanotubes/Copper Composite Film with High Performance and Waterproof Property for Underwater Motion Detection. *Compos. B. Eng.* 2023, 254, 110574.
- [16] Duan, S.; Wang, B.; Lin, Y.; Li, Y.; Zhu, D.; Wu, J. et al. Waterproof Mechanically Robust Multifunctional Conformal Sensors for Underwater Interactive Human-Machine Interfaces. *Adv. Intell. Syst.* 2021, 3 (9), 2100056.
- [17] Li, Y.; Chen, S.; Wu, M.; Sun, J., Polyelectrolyte Multilayers Impart Healability to Highly Electri-



- cally Conductive Films. *Adv. Mater.* 2012, 24 (33), 4578-4582.
- [18] Akbulut, M.; Alig, A. R. G.; Min, Y.; Belman, N.; Reynolds, M.; Golan, Y.; Israelachvili, J. Forces Between Surfaces Across Nanoparticle Solutions: Role of Size, Shape, and Concentration. *Langmuir*. 2007, 23 (7), 3961-3969.
- [19] Li, Y.; Li, W.; Sun, A.; Jing, M.; Liu, X.; Wei, L. et al. A Self-Reinforcing and Self-Healing Elastomer with High Strength, Unprecedented Toughness and Room-Temperature Reparability. *Mater. Horizons*. 2021, 8 (1), 267-275.
- [20] Lian, M.; Zheng, F.; Lu, X.; Lu, Q. Tuning the Heat Resistance Properties of Polyimides by Intermolecular Interaction Strengthening for Flexible Substrate Application. *Polymer*. 2019, 173, 205-214.
- [21] Li, H.; Li, H.; Dai, Q.; Li, H.; Brédas, J. L. Hydrolytic Stability of Boronate Ester-Linked Covalent Organic Frameworks. *Adv. Theory Simul.* 2018, 1 (2), 1700015.
- [22] Liu, Y.; Chen, T.; Jin, Z.; Li, M.; Zhang, D.; Duan, L. et al. Tough, Stable and Self-Healing Luminescent Perovskite-Polymer Matrix Applicable to all Harsh Aquatic Environments. *Nat. Commun.* 2022, 13 (1), 1338.
- [23] Bian, M.; Qian, Y.; Cao, H.; Huang, T.; Ren, Z.; Dai, X. et al. Chemically Welding Silver Nanowires Toward Transferable and Flexible Transparent Electrodes in Heaters and Double-Sided Perovskite Solar Cells. *ACS Appl. Mater. Interfaces*. 2023, 15 (10), 13307-13318.
- [24] Xiong, W.; Liu, H.; Chen, Y.; Zheng, M.; Zhao, Y.; Kong, X.; Wang, Y. et al. Highly Conductive, Air-Stable Silver Nanowire@ Iongel Composite Films Toward Flexible Transparent Electrodes. *Adv. Mater.* 2016, 28 (33), 7167-7172.
- [25] Liu, Y.; Zhang, J.; Gao, H.; Wang, Y.; Liu, Q.; Huang, S. et al. Capillary-Force-Induced Cold Welding in Silver-Nanowire-Based Flexible Transparent Electrodes. *Nano Lett.* 2017, 17 (2), 1090-1096.
- [26] Zhang, Y.; Li, M.; Qin, B.; Chen, L.; Liu, Y.; Zhang, X. et al. Highly Transparent, Underwater Self-Healing, and Ionic Conductive Elastomer Based on Multivalent Ion-Dipole Interactions. *Chem. Mat.* 2020, 32 (15), 6310-6317.
- [27] Amoli, V.; Kim, J. S.; Jee, E.; Chung, Y. S.; Kim, S. Y.; Koo, J. et al. A Bioinspired Hydrogen Bond-Triggered Ultrasensitive Ionic Mechanoreceptor Skin. *Nat. Commun.* 2019, 10 (1), 4019.